Vol 18 No 5, May 2009
1674-1056/2009/18(05)/1807-07

Chinese Physics B

© 2009 Chin. Phys. Soc.
and IOP Publishing Ltd

Studying a kind of portable ultra-bright microfocus x-ray source*

Wang Kai-Ge(王凯歌)[a)b)], Wang Lei(王 雷)[c)], and Niu Han-Ben(牛憨笨)[b)†]

[a)] *Institute of Photonics & Photonic Technology, Northwest University, Xi'an* 710069, *China*
[b)] *Institute of Optoelectronics, Shenzhen University, Shenzhen* 518060, *China*
[c)] *Xi'an Institute of Applied Optics, Xi'an* 710065, *China*

(Received 19 September 2008; revised manuscript received 15 October 2008)

This paper studies the properties of a kind of portable ultra-bright microfocus x-ray source with the Monte-Carlo method in detail. The new x-ray source consists of an electron-emission system, an electrostatic focusing system and a metal target. A crystal Lanthanum Hexaboride cathode, a Wehnelt grid and an extracted electrode compose the triode electrode electron-gun system. Two equal radius cylinder electrodes form the focusing system. The key factors determining the focus properties of the electron beam such as the ratio $D_{\rm w}/H$, grid bias $V_{\rm g}$, and the properties of the extracted electrode are numerically studied. The calculated results reveal that when $D_{\rm w}/H$, $V_{\rm g}$, the length of the extracted electrode, and the distance between the grid and the extracted electrode equals 5, –0.6 kV, 10 mm, and 8 mm respectively, the electron beam focal spot can be concentrated down to 9 μm in radius and a reasonable focal length about 72.5 mm can be achieved, at the same time, the cathode emission currents can be as high as 30 mA.

Keywords: microfocus x-ray source, high brightness, micro-focal spot, Monte-Carlo method
PACC: 0785, 4180D

1. Introduction

A microfocus x-ray source with high-brightness is the primary component for modern x-ray optics such as x-ray microscopy, x-ray CT, x-ray phase contrast imaging and micro x-ray absorption spectroscopy.[1−4] These microfocus x-ray sources enable researchers to achieve high spatial resolution and high magnification in the studies of biology, biomedicine, material science, and life science. In the last two decades, microfocus x-ray sources have been greatly developed in the types of operating instruments as well as their capabilities.[5−8] However, potential applications of most current high brightness microfocus x-ray sources, e.g., the synchrotron light source and the laser plasma x-ray source, are restricted to research laboratories because of their large size, high costliness and complex working conditions.[9−11]

X-ray photons can be radiated by a beam of high-energy electrons bombarding upon a metallic target (anodes). Further, x-ray photons radiating with a microscale focus can become true by a beam of high energy electrons with a microscale focal spot. This is one of the most effective and simplest methods which has been widely adopted in the manufacture of microfocus x-ray sources and has made fruitful achievement. However, most current commercial portable microfocus x-ray sources are unable to achieve hard x-ray emission with high luminance simultaneously.[12,13] In order to reduce the focal spot and meanwhile increase the intensity of electron beam, scientists have exploited some new approaches to improve the focus of the x-ray and utilize new materials as emission cathodes.[14,15] Researchers have displaced thermal electron emission with electric field emission in conventional x-ray tubes, and employed carbon nanotubes as emitting cathodes in these high-field emitting x-ray tubes. Reference [16] reported that Beg and his colleagues added a focusing electrode behind the grid in a traditional x-ray tube to obtain small focus.[16] Previously, we have also theoretically and experimentally studied a kind of microfocus x-ray source which radiated hard x-ray photons with a focal spot size about 10 μm,[17,18] the smaller emission current (∼50 μA) of the prototype source was regrettably imperfect.

*Project supported by the Major Program of the National Natural Science Foundation of China (Grant No 60532090), and the National Natural Science Foundation of China (Grant No 60771048).
†E-mail: HBNiu@szu.edu.cn

In order to carry out more emission of x-ray photons, high intensity electrons are necessary. Thus, the key issues of an ultra-bright microfocus x-ray source are following: the first is to employ an excellent electron emitting source that produces enough electrons, and the second is to have a powerful focusing system to concentrate electrons down to a microscale spot. For integrating a unitive x-ray source, it is another compulsory subject to match the two parts mentioned above and other components precisely. Here, we will introduce and study properties of the portable ultra-bright microfocus x-ray source which we designed with the Monte-Carlo method.

2. Structure of the microfocus x-ray tube

The designed portable x-ray tube is composed of three parts, an electron-beam emission system, an electrostatic focusing system and a metal target. The emission system is a triode electrode gun which consists of a cathode, a Wehnelt grid and an extracted electrode. The focusing system consists of two equal radius cylindrical electrodes. Figure 1 is the schematic drawing of the microfocus x-ray source.

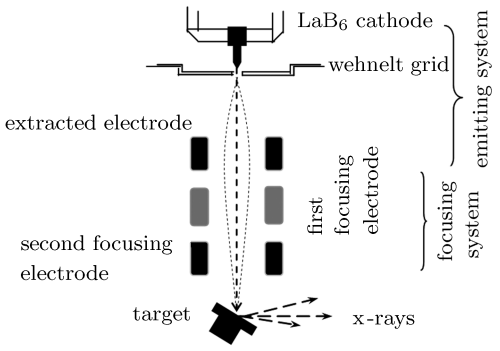


Fig.1. Sketch diagram of the microfocus x-ray tube.

There are many advantages to our microfocus x-ray source. On one hand, the triode electrode emission system includes a Wehnelt grid and an extracted electrode, the voltage of the extracted electrode can be as high as 100 keV, so there is a higher electric field in the electron gun system with which the space charge effects at the cathode tip can be overcome and thus the high brightness cathode can be maintained; and more, the electron currents emitted from the cathode can be controlled easily by adjusting the small value of the grid bias. On the other hand, two equal radius cylindrical electrodes as the focusing system will not only ensure the x-ray photons radiate with a micro scale focal spot but also benefit the whole x-ray tube portability.

A Lanthanum Hexaboride crystal (LaB_6, Kimball Physics Inc.) was chosen as the cathode in our x-ray source, mainly because it has high beam currents and thousands of hours ($\sim$5000 h) of stable operation. The emission area of the LaB_6 crystal surface is the first factor to be considered in the study. However, it is conflictive. The emission area of the LaB_6 crystal is fundamental for the cathode emission currents. There is a higher emission current with a bigger emission area. In contrast, the size of the cathode emitting area influences the properties of the electron beam focus, with a bigger emission area, it is difficult to achieve a smaller focal spot. Taking into account the case of our project, the emission currents must approach 30 mA, so we chose a reasonable LaB_6 crystal cathode with emission area as big as 330 μm in diameter.

Besides the area of cathode surface, there are other factors, such as LaB_6 cathode temperature, the ratio D_w/H (the ratio of the Wehnelt grid aperture diameter D_w to the cathode setting height H, the height H is defined as the distance between the cathode emitting surface and the outer surface of the Wehnelt aperture) and grid bias V_g, which determine the amount of the electrons bombarding upon the anodic target, and thus influence the intensity of x-ray photons. In addition, the properties of the electrostatic focusing system, such as the voltage and spatial position and geometric configuration of every electrode, influence the properties of the focus strongly. The functions of these factors will be discussed in the next section.

3. Numerical calculation and discussion

The Monte-Carlo method was used to track the trajectories of electrons within the whole x-ray tube, and the numerical finite element method (FEM) was utilized to calculate the distribution of electrical-field intensity and potential of every point. In the calculation, we made several reasonable approximations. Firstly, electron emission occurs only from the top facet of the LaB_6 crystal facing the anode side, and the emission exhibits a uniform distribution from the

area of the truncation. Secondly, the LaB_6 cathode tip was centred in the Wehnelt grid accurately, and the other components have a stringent alignment, so the tube maintains a coaxial symmetric system.

We developed software written with the MATLAB language, tracing an amount of 10^4 electrons emitting in the tube, then the distribution of electrons on the anode surface was statistically studied. We have successfully used this software in our previous work where we designed and fabricated a prototype of the microfocus x-ray source. The experimental results of the electron beam focus were very much in accord with the calculated data.[17,18] The electron optical system of the x-ray tube is of perfect coaxial symmetry. Equations used in the three-dimensional reference coordinates are

$$\ddot{X} = \frac{e}{m}E_x,$$
$$\ddot{Y} = \frac{e}{m}E_y,$$
$$\ddot{Z} = \frac{e}{m}E_z, \qquad (1)$$

where E_r (E_x, E_y) and E_z stand for the radial and axial field intensity, respectively.

We calculated the trajectory of every electron emitted from the top surface of the LaB_6 crystal cathode and then statistically analysed the electron local position bombarded on the anode. The results of electron trajectories within the x-ray tube revealed that electrons are launched from the LaB_6 crystal surface, then these electrons move forward and form a small cross spot near the grid aperture under electrostatic field (the cathode emission system approximated a convex lens). Then, electrons are accelerated into the electrostatic-field focusing system and strongly concentrated. Finally, these electrons with high kinetic energy bombard upon the metal target to irradiate the x-ray photons. The objective of the following is to discuss the properties of the electron beam focus, e.g., the focal spot size and the focal length.

Figure 2 is a group of charts showing electron beam focal spot size versus the ratio D_w/H. Figure 3 is a group of charts of electron beam focal length versus the ratio D_w/H. In these cases, the focusing system frameworks and pole potentials are steady. In Figs.2 and 3, the first focusing electrode voltage is 10 kV, 12.5 kV, 15 kV, 17.5 kV, and 20 kV respectively, which is marked by a reversed triangle, diamond, circle, pentacle, and triangle. The solid curves are guides for the eye.

It can be noticed that the focal spot size and focal length of the electron beam are influenced strongly by

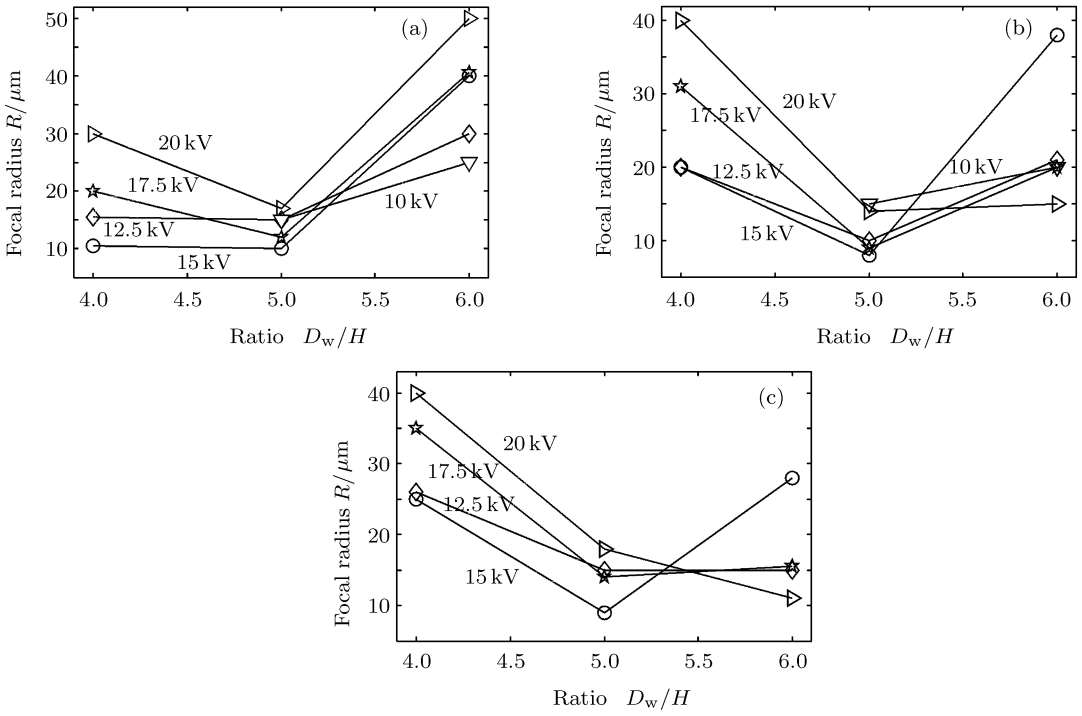


Fig.2. The electron beam focal spot size versus the ratio D_w/H for different grid bias. The grid bias V_g is (a) –0.5 kV, (b) –0.6 kV, and (c) –0.7 kV, respectively.

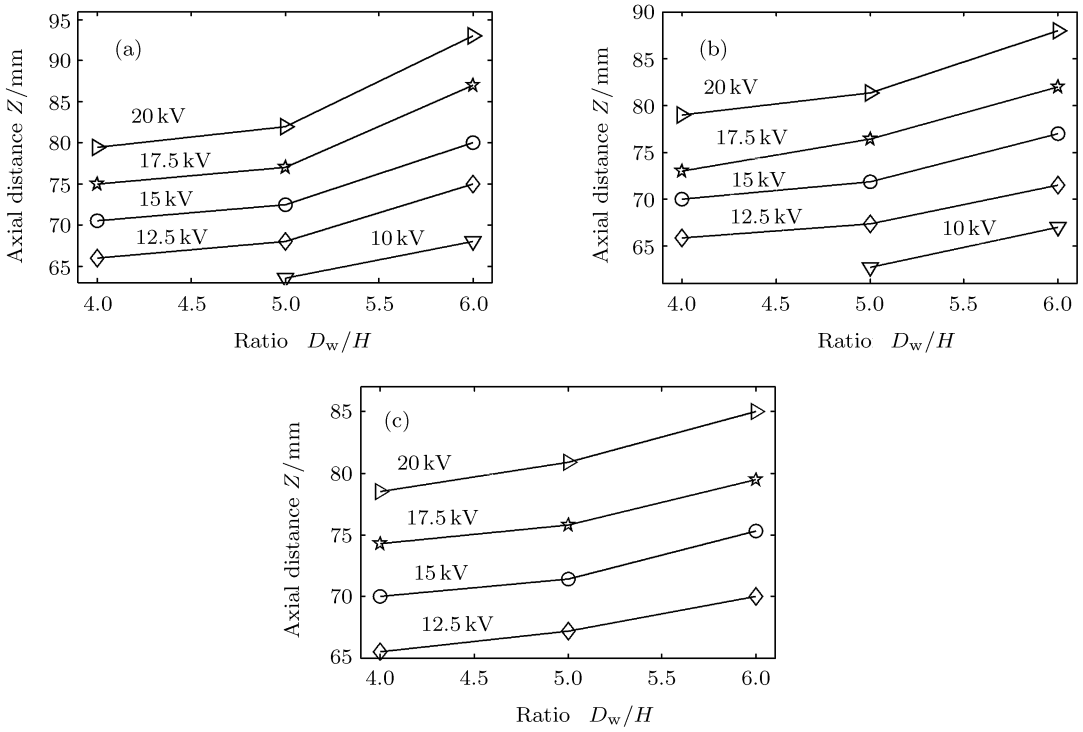


Fig.3. The electron beam focus length versus the ratio D_w/H for different grid bias. The grid bias V_g is (a) –0.5 kV, (b) –0.6 kV, and (c) –0.7 kV, respectively.

the value of ratio D_w/H. Figure 2 reveals that the focal spot size is changed nonlinearly with the ratio D_w/H, however, an optimal value for the minimal focal spot size exists. In all sorts of conditions, a smaller focal spot can be always achieved when the ratio D_w/H equals 5. On the other hand, the focal length is directly proportional to the ratio D_w/H, that is, the bigger the value of D_w/H the bigger the focal length. It can also be noticed from Fig.3 that the focal length changes evidently as the voltage of the first focusing electrode increases from 10 kV to 20 kV while the grid bias V_g maintains a constant value.

Figure 2 just shows the better focal spot size of the electron beam when the value of ratio D_w/H varies from 5 to 7. In fact, we have also calculated the focus under other working conditions, e.g., ratio values equal to 2, 3, 4, 8, and 9. The calculated data are complex. When the ratio $D_w/H \leq 3$, results show that only a few of the electrons can arrive at the target surface (data not shown). The reason is that the grid aperture in these cases is too small to transfer electrons and the grid wall blocks a large amount of electrons. Another dramatic phenomenon is that there is no electron beam crossing spot near the grid pinhole when $D_w/H \geq 8$, thus there is no effect of electrons pre-focusing, and the ultimate electron beam focusing radii are all bigger than 100 μm (data not shown).

The electron beam focal length is a key factor which determines the volume of the microfocus x-ray source. Notice that the focal length increases with the increase of voltage applied to the first focusing electrode, no matter what the value of ratio D_w/H or grid bias is. In Fig.3, it can be noted that the focal length increases with the increase of D_w/H though this change is not prominent.

Figure 4 shows the electron beam focal spot size versus grid bias value as the ratio $D_w/H = 5$. Figure 5 shows the electron beam focal spot size versus the first focusing electrode voltage. The properties of the electron beam focus are dependent on the grid bias and the voltage of the first focusing electrode. Figure 4 shows that the smallest focal spot size can be achieved when the voltage of the first focusing electrode is 15 kV. In Fig.5, it can be noticed that there is a smaller focal spot when the grid bias value is $V_g = -0.6$ kV no matter what the value of the first focusing electrode potential is.

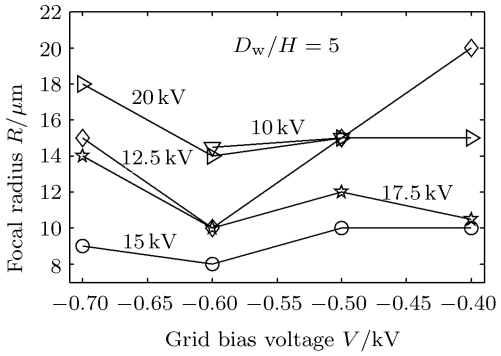


Fig.4. The electron beam focal spot size versus grid bias voltage for different values of the first focusing electrode voltage.

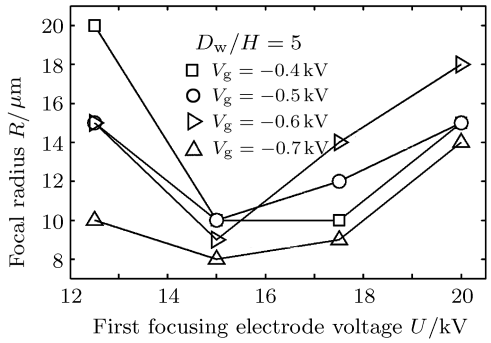


Fig.5. The electron beam focal spot size versus the first focusing electrode voltage for different values of grid bias.

As a united system, two parts of the electron beam emission system and the focusing system should be functionally and integrally coupled. The extracted electrode acts as the concatenated bridge between these two sub-systems. The properties of the extracted electrode such as the spatial position and geometric configuration are important for the properties of electron focus. Figure 6 shows the electron beam focal spot size varying with the length of the extracted electrode. Figure 7 shows the focal spot sizes varying with the spatial position of the extracted electrode. In the calculation, other parameters such as the ratio D_w/H, radius of extracted electrode R_{v1}, grid bias, and the voltage of the first focusing electrode are 5, 1 mm, –0.6 kV, and 15 kV, respectively.

In the cases shown in Figs.6 and 7, the radius of the extracted electrode (R_{v1}) is 1 mm. For choosing the optimal extracted electrode, we have analysed the properties of electron beam focus under various extracted electrode radii ($R_{v1} = 0.5$ mm, 1 mm, 1.5 mm, 2 mm, etc.); the results reveal that the focal spot sizes are approximately equivalent when $R_{v1} = 1$ mm and $R_{v1} = 1.5$ mm. However, when $R_{v1} = 0.5$ mm or 2 mm, the focal spot radii are bigger than 10 μm and the focal length are larger (data not shown).

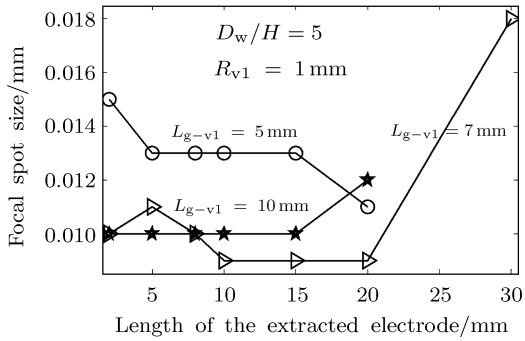


Fig.6. The electron beam focal spot size versus the length of the extracted electrode for different values of distance between the grid and extracted electrode L_{g-v1}.

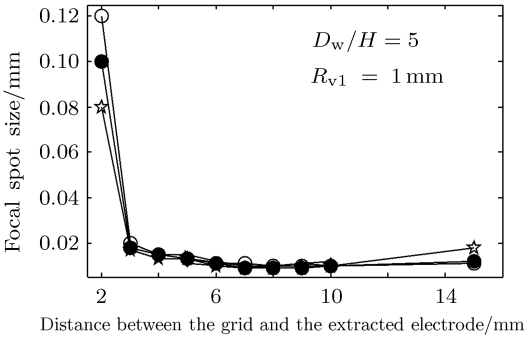


Fig.7. The electron beam focal spot size versus the distance between the grid and the extracted electrode. Length of the extracted electrode is 2 mm, 5 mm, 8 mm, 10 mm, 15 mm, and 20 mm, which is marked by an open circle, square, diamond, pentacle, filled circle, and triangle, respectively.

In Fig.7, it is important to note that the radii of focal spots are ∼10 μm when the distance between grid and extracted electrode (L_{g-e}) is ranged from 6 mm to 10 mm. In fact, the focal spot radii are statistically stabilized 9 μm when the length L_{g-e} is ranged from 7 mm to 9 mm. We have numerically analysed the properties of electron beam focus when the length of the extracted electrode (L_e) is ranged from 2 mm to 20 mm (data not shown) when the length L_{g-e} increases from 2 mm to 15 mm (partial data shown in Fig.6). We noticed that the focal spot size has a stabilized radius when $L_e = 10$ mm.

Figure 8 shows the electron beam focal length varying with the length of the extracted electrode. It can be noted that the focal length increases with the increase of the length of the extracted electrode.

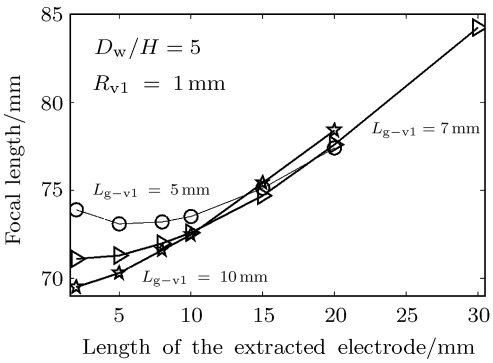


Fig.8. The electron beam focal length versus the length of the extracted electrode. The voltage of the first focusing electrode is 15 kV. L_{g-v1} is 5 mm, 7 mm, and 10 mm which is marked by a circle, triangle, and pentacle, respectively.

In order to estimate the properties of electron beam focus, we also calculate the focal spot size and the focal length changing with the change of geometric configuration (length of extraction electrode) and the spatial position (distance between grid and extraction electrode) when the potential of the first focusing electrode has other values, e.g., 13 kV, 14 kV, 16 kV, 17 kV, and 17.5 kV (data not shown). Comparing the calculated data, we find that the results reveal that the focal spot size and the focal length are all bigger than in the case when the first focusing electrode is 15 kV.

In addition, we studied the focus properties of an electron beam in the x-ray tube when the focusing system only comprises one electrode. The calculated results reveal that the focal spot radii are all no less than 80 μm (data not shown).

Table 1. The electron beam focus versus the extracted electrode (D_w/H = 5, L_{vg} = 0.1mm, $V_g = -0.6$kV, $V_1 = V_3 = 10^5$kV, $V_2 = 1.5 \times 10^4$kV).

L_{v1-vg} /mm	L_{v1} /mm	R_{v1} /(mm)×0.1	focal spot size /(radius mm)±0.001	focal length /(mm)±0.001	cross spot /(radius mm) ±0.001
8	5	10	0.010	70.9	0.013
		15	0.010	70.9	0.013
	10	10	0.009	72.5	0.013
		15	0.009	72.5	0.013
	15	10	0.009	74.8	0.013
		15	0.009	74.9	0.013

We have studied the properties of the electron beam focus in various structures of x-ray tube with different ratio D_w/H, grid bias V_g and parameters of the extracted electrode, and the results indicate that the minimal focal spot is able to condense to 9 μm in radius when the ratio $D_w/H = 5$ and $V_g = -0.6$ kV and $L_{g-e} = 8$ mm and $L_e = 10$ mm. The properties of the extracted electrode contributing to the focal spot size and the focal length are shown in detail in Table 1, where the mean error is about 0.5×10^{-3}. We noticed that the focal spot size of the electron beam focused on the anode target is similar when the distance between the grid and the extracted electrode changed from 7 mm to 9 mm; in these cases, the length and the radius of the extracted electrode are constants, 10 mm and 1 mm, respectively.

In our new microfocus x-ray source, a crystal LaB_6 cathode is chosen as the electron emitting cathode due to its many superior qualities, the greatest of which is its great emission current. Thus, we can realize x-ray photons emitting with ultrahigh brightness. A Wehnelt grid is chosen because this component can easily make the microfocus x-ray source work in pulse mode which is beneficial to the acquisition of x-ray images for moving objects. The unique features of configuration and high potential of the extracted electrode can not only greatly accelerate the electrons but also avoid the space charge effects in the electron emission system. The focusing system consisting of a couple of equal radius cylindrical electrodes avoids several fundamental disadvantages of conventional microfocus x-ray source such as unwieldiness and big spot size. In the new x-ray source, the energy of the electrons can be accelerated to 100 keV without defocusing, hence, hard x-ray irradiation with a microscale focus can be obtained.

4. Conclusion

A kind of portable ultra-brightness microfocus x-ray source was designed and numerically analysed. The x-ray tube consisted of an electron-emission system, an electrostatic focusing system and a metal target. A crystal Lanthanum Hexaboride cathode, a Wehnelt grid and an extracted electrode composed the electron emitting system. Two equal radius cylindrical electrodes made the focusing system. The Monte-Carlo simulation results indicated that the novel x-ray source can achieve hard x-ray photons (100 keV) emission with a focal spot 9 μm in radius. At the same time, the LaB_6 crystal cathode emission current can be as high as 30 mA. These results offer the promise of manufacture and accomplishment of an ultra-bright microfocus x-ray source which is smaller, portable, more cost-effective and more powerful. This kind of x-ray source will be very useful in the fields of x-ray optics fundamental research and medical imaging. As an extension of this work, we are currently working on a kind of novel structural target system for microfocus x-ray photons irradiating with high spatial coherence.

References

[1] Jenneson P M, Atkinson E C, Wai P and Doran S J 2004 *J. Physics*: *Conference Series* **3** 257

[2] Chen M, Chen J W, Gao H Y, Lu P X and Xu Z Z 2003 *Chin. Phys.* **12** 55

[3] Huang W X, Yuan Q X, Tian Y L, Zhu P P, Jiang X M and Wang J Y 2005 *Acta Phys. Sin.* **54** 677 (in Chinese)

[4] George G N, Doonan C J, Rothery R A, Boroumand N and Weiner J H 2007 *Inorg Chem.* **46** 2

[5] Cameron R, Huddlestone H and Ketcham R A 2005 *American Mineralogist.* **90** 1

[6] Zeng Z Z and Qiu A C 2004 *Chin. Phys.* **13** 201

[7] Takeyoshi T 2001 *Analytical Sciences* **17** i139

[8] Ozawa S, Wakasugi M, Okamura M, Katayama T, Koizumi T and Serata M 2004 *Rev. Sci. Instrum.* **76** 1579

[9] Hiroyuki U, Keníchi T and Hiroshi T 2007 *Jpn. J. Appl. Phys.* **46** 3096

[10] Cherry S R 2004 *Phys. Med. Biol.* **49** R13

[11] Liu L X, Du G H, Hu W, Xie H L and Xiao T Q 2007 *Acta Phys. Sin.* **56** 4556 (in Chinese)

[12] Lutterodt K E, Ablett J, Stein A, Kao C C, Tennant D, Klemens F, Taylor A, Jacobsen C, Gammel P, Huggins H, Bogart G, Ustin S and Ocola L 2003 *Opt. Exp.* **11** 919

[13] www.OxfordxTG.com

[14] Yue G Z, Qiu Q, Gao B, Cheng Y, Zhang J, Shimoda H, Chang S, Lu J P and Zhou O 2002 *Appl. Phys. Lett.* **81** 355

[15] Zhang J, Cheng Y, Lee Y Z, Gao B, Qiu Q, Lin W L, Lalush D, Lu J P and Zhou O 2005 *Rev. Sci. Instrum.* **76** 094301

[16] Beg F N, Stephens R B, Xu H W, Haas D, Eddinger S, Tynan G, Shipton E, DeBono B and Wagschal K 2006 *Appl. Phys. Lett.* **89** 101502

[17] Wang K G, Guo B, Guo J, Li J, Yang Q, Kuo X, Zhou J and Niu H 2007 *Proc. SPIE.* **6279** 627914

[18] Wang K G, Wang L, Liu W and Niu H 2006 *Chin. Phys. Lett.* **23** 2368